International Institute of Welding
A world of joining experience

Optimization and comparison of welded compressed columns

Károly JÁRMAI[1], Máté PETRIK[2]

[1,2]University of Miskolc, H-3515 Miskolc, Hungary

[1]Professor, Dr.sci.techn. jarmai@uni-miskolc.hu, [2]PhD student, vegypet@uni-miskolc.hu

IIW ANNUAL ASSEMBLY 2016, MELBOURNE

Abstract

Stability is one of the most important problems in the design of welded metal structures, since the instability causes in many cases failure or collapse of the structures. The aim of the present study is to show the minimum mass design procedure for welded steel I- and box columns loaded by a compression force. The normal stresses and overall stability are calculated for pinned columns. The dimensions of the I- and box columns are optimized by using constraints on overall stability, local buckling of webs and flanges. The different design rules and standards, like Eurocode 3, Japan Railroad Association (JRA), American Petroleum Institute (API), and American Institute of Steel Construction (AISC) have been compared. The calculations are made for different loadings, column length and steel grades. The yield stress varies between 235 and 690 MPa. The optimization is made using the Generalized Reduced Gradient (GRG2) method in the Excel Solver.

Keywords: welded column, structural optimization, overall stability constraint, minimum mass

1 Introduction

The world view shows the complexity of problems and the differences between the solutions and design rules. From many books on structural stability it is worth mentioning the following: Kollár and Dulácska (1984) about the stability of shells, Petersen (1980) with many numerical examples, a detailed Japanese handbook on stability Handbook (1970), Chen and Li (1991) about the stability of frames, Rondal et al (1992) about the stability of structures with hollow sections, Waszczyszyn et al. (1994) treat the stability problems by finite element methods.

In the recent years there are many publications dealing with special cold-formed steels like lipped channel columns with and without stiffening (Anbarasu and Murugapandian 2016, Manikandan and Arun 2016, Wang et al. 2016, Kumar and Kalyanaraman 2014). The local–distortional interaction effects is also can be important (Martins et al. 2015ab). High strength steel applications show, that they are getting cheaper (Lian et al. 2015, Wang et al. 2014). The calculation of this phenomena is also refined using complex finite strip method (Naderian and Ronagh 2015). The interactions of different stability modes are also very important (Dinis and Camotim 2015, He et al. 2014, Dinis et al. 2014, Kwon 2014, Kwon and Seo 2013, Young et al. 2012, Dubina et al. 2013). Cold-formed steel perforated sections in compression have a special behaviour (Crisan et al. 2012). Optimization of these cold-formed steel column sections shows the importance of reducing mass or cost (Gilbert et al. 2012). There are softwares to make these calculations (Bebiano et al. 2008).

2 Compression members

2.1 Flexural buckling

The development in the calculation of overall buckling of compressed struts shows clearly how the model was refined considering the fabrication aspects.

In the first phase Euler (1778) has solved the differential equation for a straight strut to obtain the critical force

$$F_E = \pi^2 EI_x / (KL)^2 \qquad \text{or stress} \qquad \sigma_E = \pi^2 E / \lambda^2 ; \quad \lambda = KL / r \qquad (1)$$

where $r = \sqrt{I_x / A}$ is the radius of gyration, K is the effective length factor, A is the cross-sectional area, E is the modulus of elasticity, L is the strut length, I_x is the moment of inertia. Figure 1 shows

that the Euler hyperbola is valid only in the elastic range, when $\sigma \leq \sigma_0$ where σ_0 is the elastic limit stress.
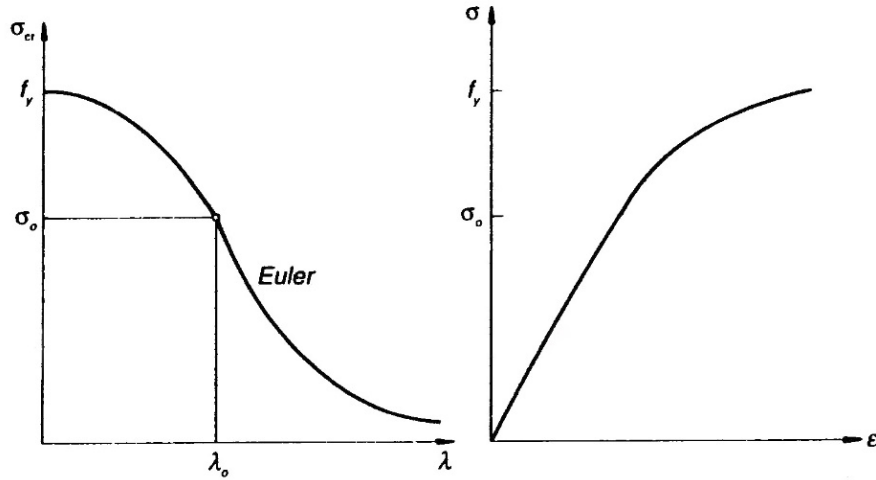

Figure 1. Euler curve, plastic and elastic overall buckling

Later the plastic buckling has been described by several authors.

In the second phase Ayrton and Perry (1886) have taken into account the initial crookedness as regards the initial imperfections. It is worth describing their model since this model is the basis of the EC3 overall buckling formula.
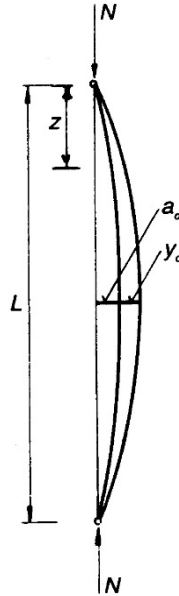

Figure 2. The Ayrton-Perry model for initially curved column and the second order elastic deformation

The differential equation for a centrally compressed strut with pinned ends and a sinusoidal initial crookedness (Fig. 2)

$$a = a_0 \sin(\pi z / L) \tag{2}$$

is

$$\frac{d^2 y}{dz^2} = -\frac{M}{EI_x} = -\frac{N(a+y)}{EI_x} \tag{3}$$

N is the compressive force. Searching the solution in the form of

$$y = y_0 \sin(\pi z / L) \tag{4}$$

we get

$$y_0 = \frac{a_0}{F_E / N - 1} \tag{5}$$

The overall buckling formula can be derived on the basis of the check for eccentric compression

$$\frac{N}{A} + \frac{N(a_0 + y_0)}{W_x} \le f_y \tag{6}$$

In the third phase the effect of residual welding stresses has been considered. The European overall buckling curves have been determined for various welded sections based on statistical evaluation of many test results (Beer and Schulz 1970). The tests have shown that the residual welding stresses significantly influence the buckling strength mainly in the case of welded I-sections since compressive residual stresses occur at the edges of the flanges decreasing the buckling strength.

EC3 applies the formula proposed by Maquoi and Rondal (1978). This formula can be derived from Eq. (6) considering one parameter which expresses the effect of initial imperfection and residual welding stresses as follows.

With notations of

$$\sigma = N / A; \sigma_E = F_E / A; \eta_b = a_0 A / W_x$$

Eq.(6) can be written in the form

$$\left(f_y - \sigma\right)\left(\sigma_E - \sigma\right) = \eta_b \sigma \sigma_E \tag{7}$$

This equation can be transformed using the following relationships

$$\sigma / f_y = \chi; \sigma_E / f_y = \pi^2 E / \left(f_y \lambda^2\right) = 1 / \overline{\lambda}^2 \tag{8}$$

$$\overline{\lambda} = \lambda / \lambda_E; \lambda_E = \pi \sqrt{E / f_y}$$

to obtain

$$\left(1 - \chi\right)\left(\frac{1}{\overline{\lambda}^2} - \chi\right) = \frac{\chi \eta_b}{\overline{\lambda}^2} \tag{9}$$

This leads to the following quadratic equation

$$\chi^2 - \left(1 + \frac{\eta_b}{\overline{\lambda}^2} + \frac{1}{\overline{\lambda}^2}\right)\chi + \frac{1}{\overline{\lambda}^2} = 0 \tag{10}$$

The solution of Eq. (10) is

$$\chi = \frac{\phi - \sqrt{\phi^2 - \overline{\lambda}^2}}{\overline{\lambda}^2} = \frac{1}{\phi + \sqrt{\phi^2 - \overline{\lambda}^2}} \tag{11}$$

where

$$\phi = 0.5\left(1 + \eta_b + \overline{\lambda}^2\right) \qquad \text{and} \qquad \eta_b = \alpha\left(\overline{\lambda} - 0.2\right)$$

For $\overline{\lambda} \le 0.2$ it is $\chi = 1.$

α is the imperfection factor given for various buckling curves in Table 1.

Table 1 Imperfection factors

Buckling curve	a	b	c	d
Imperfection factor	0.21	0.34	0.49	0.76

Selection of buckling curve for cross-sections according to EC3:

a - for hot rolled hollow sections

b - for cold formed hollow sections, welded box sections, welded I-sections buckling about the strong axis with flange thickness smaller than 40 mm,

c - for welded I-sections buckling about the weak axis with a flange thickness smaller than 40 mm, for welded I-sections buckling about the strong axis with a flange thickness larger than 40 mm, for U-, L-, T- and solid sections,

d - for welded I-sections buckling about the weak axis flange thickness larger than 40 mm

The strut should be checked for

$$N \le \chi A f_y / \gamma_{M1} \tag{12}$$

where $\gamma_{M1} = 1.1$ is the safety factor for buckling.

It should be mentioned that the EC3 formula is too complicated for design (non-computerized optimization) purposes. There exist other column curves used in other countries which can be applied instead of EC3 curves. Figure 3 shows some other buckling curves in addition to the EC3 curve "b". It can be seen that the curve of the Japan Railroad Association (JRA) gives values near the EC3 curve "b". The JRA curve is described by the following formulae

$$\chi = 1 \qquad \text{for} \qquad \overline{\lambda} \le 0.2$$

$$\chi = 1.109 - 0.545\overline{\lambda} \qquad \text{for} \qquad 0.2 \le \overline{\lambda} \le 1 \tag{13}$$

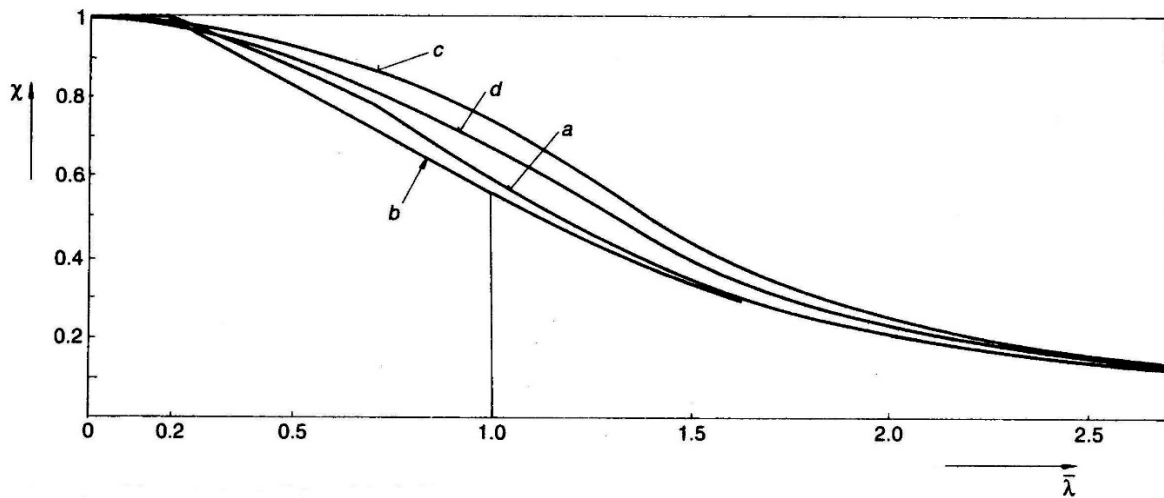$$\chi = 1/\left(0.773 + \overline{\lambda}^2\right) \qquad \text{for} \qquad \overline{\lambda} \ge 1$$

Figure 3. Overall buckling curves according to a) EC3; b) JRA; c) API; d) AISC

The curve of the American Petroleum Institute (API) is defined by

$$\chi = 1 - 0.25\overline{\lambda}^2 \qquad \text{for} \qquad 0 \le \overline{\lambda} \le 1.41 \qquad (14)$$

$$\chi = 1/\overline{\lambda}^2 \qquad \text{for} \qquad \overline{\lambda} \ge 1.41$$

The curve of the American Institute of Steel Construction (AISC) mainly for round tubes is given by

$$\chi = 1 - 0.091\overline{\lambda} - 0.22\overline{\lambda}^2 \qquad \text{for} \qquad \overline{\lambda} \le 1.41 \qquad (15a)$$

$$\chi = 0.015 + 0.834/\overline{\lambda}^2 \qquad \text{for} \qquad \overline{\lambda} \ge 1.41 \qquad (15b)$$

In the fourth phase the experiments carried out on thin-walled rectangular hollow section compression struts in the University of Liege have shown the interaction of local buckling of plate elements and the overall buckling. When the plate element loaded in maximum compressive stress buckles, the overall buckling strength decreases. Braham et al (1980) have proposed a reduction factor for this case which is included in EC3 as follows: Eq. (12) is modified to

$$N \le \beta_A \chi A f_y / \gamma_{M1} \qquad \text{and} \qquad \overline{\lambda} = \lambda \sqrt{\beta_A} / \lambda_E \qquad (16)$$

where $\beta_A = 1$ for cross-sections of class 1,2 and 3, $\beta_A = A_{eff}/A$ for class 4 cross-sections. The area of the effective cross-section A_{eff} can be calculated using the effective width formulae for compression elements.

For aluminium alloy compression members the rules of BS 8118 (1991) can be used. This standard contains overall buckling formulae which are the same as the EC3 formulae. The initial imperfection factor should be taken as follows: for symmetric sections unwelded $\alpha = 0.2$, welded 0.45.

Summarizing it can be concluded that the development of the strength calculation leads from the Euler's differential equation to the EC3 formulae which take into account the initial imperfections, residual welding stresses and the interaction of local and overall buckling.

Note that the interaction of two instability phenomena plays an important role in the optimum design.

The effective length factor K expresses the effect of end restraints. The classical values are given in Figure 4. Different values are used in frame and truss analysis.
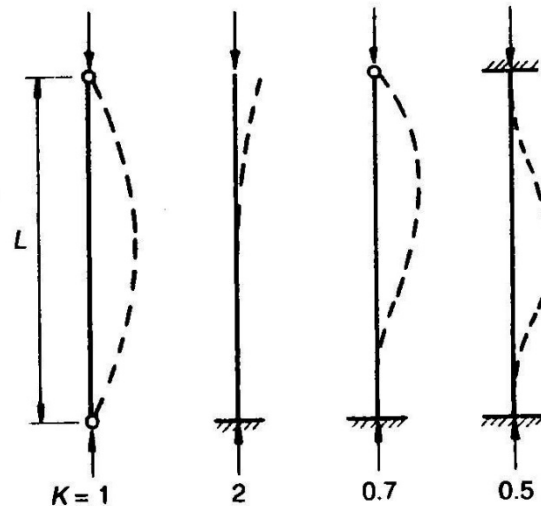

Figure 4. The buckling length values (K) for different end conditions

Note that in the case of loads fluctuating in tension-compression the strut should be designed also against fatigue failure of its connections (e.g. welded connections to gusset plates or other structural members).

2.2 Limiting plate slendernesses

It is useful for design to define limiting plate slendernesses, since in this case it is not necessary to calculate with effective widths and the cross-section can be categorized in class 3. In the optimum design the local buckling constraints can be expressed by means of the limiting plate slendernesses. For the definition the basic formula of Eq. (17) can be used:

$$\sigma_{cr} = k_\sigma \frac{\pi^2 E}{12(1-v^2)} \left(\frac{t}{b}\right)^2 \geq \sigma_{max} \qquad (17)$$

where σ_{max} is the design stress, usually the yield stress, but in the case when the deflection or the fatigue constraint is active, the actual maximum static or fatigue stress can be used. From Eq. (17) one obtains for limiting slenderness

$$\left(\frac{b}{t}\right)_L = \sqrt{\frac{k_\sigma \pi^2 E}{12(1-v^2)\sigma_{max}}} \qquad (18)$$

In EC3 the stress of 235 MPa is selected for basis and the ratio of $\varepsilon = \sqrt{235/f_y}$ is introduced. With values $E = 2.1*10^5$ MPa and $v = 0.3$ Eq.(18) takes the form of

$$\left(\frac{b}{t}\right)_L = 28.42\varepsilon\sqrt{k_\sigma}\sqrt{\frac{f_y}{\sigma_{max}}} \qquad (19)$$

For a simply supported uniformly compressed plate (e.g. a flange of a box girder) $k_\sigma = 4.0$ and

$$(b/t)_L = 56.84\varepsilon\sqrt{f_y/\sigma_{max}} \qquad (20)$$

Since this value does not contain the effect of initial imperfections and residual welding stresses, EC3 gives instead of 56.84 the value of 42.

For a uniformly compressed plate with three edges simply supported and the fourth free (e.g. half width of flanges of a welded I-section) with $k_\sigma = 0.456$

$$(b/2t)_L = 19.19\varepsilon \qquad \text{in EC3} \qquad 14\varepsilon \qquad (21)$$

For a simply supported plate loaded in bending (web of a doubly symmetric welded I-beam) $k_\sigma = 23.9$

$$(h/t_w)_L = 138.94\varepsilon \qquad \text{in EC3} \qquad 124\varepsilon \qquad (22)$$

3 Optimization

Requirements for modern load-carrying structures are the safety, fitness for production and economy. In the optimum design procedure the safety and fitness for production are guaranteed by fulfilling of design and fabrication constraints, and the economy is achieved by minimization of the mass, or the cost function.

3.1 Objective function

The objective function to be minimized selected in this study is the mass of the I- or box column (Fig. 5).
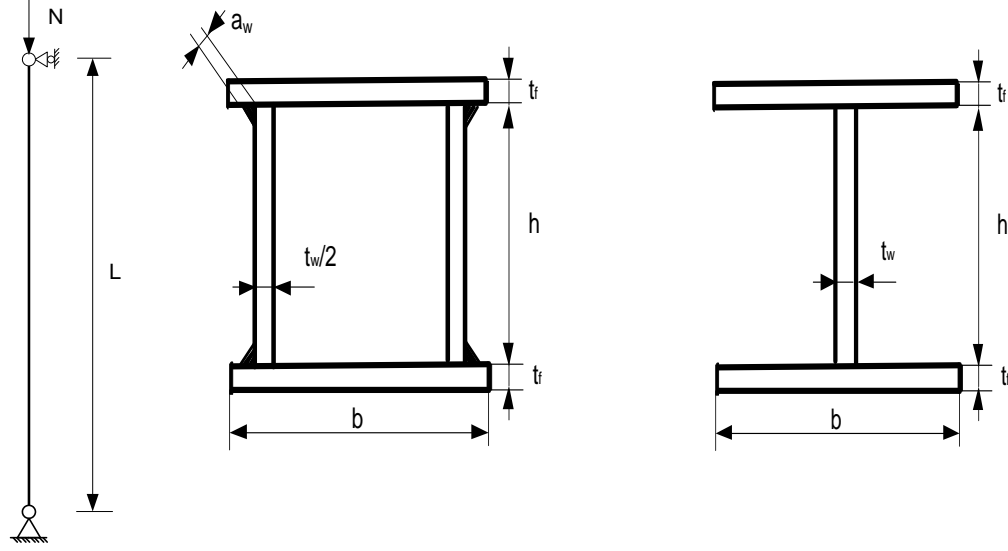
Figure 5. The welded box and I-column

The cross section area is as follows for both the I- and the box column

$$A = ht_w + 2bt_f \tag{23}$$

3.2 Constraints

Constraint of overall buckling is according to the standard, or design guide

$$N \le \chi A f_y / \gamma_{M1} \tag{24}$$

For the buckling parameter see Eqs. (13-15 and 11).

Constraint on local buckling of web for the box column

$$\frac{h}{t_w/2} \le \frac{1}{\beta}; \quad \text{or} \quad t_w \ge 2\beta h \tag{25}$$

Constraint on local buckling of web for the I-column

$$\frac{h}{t_w} \le \frac{1}{\beta}; \quad \text{or} \quad t_w \ge \beta h \tag{26}$$

where

$$1/\beta = 42\varepsilon; \varepsilon = \sqrt{\frac{235}{f_y}} \tag{27}$$

Constraint for local buckling of compressed upper flange of box column

$$\frac{b}{t_f} \le \frac{1}{\delta} = 42\varepsilon, \quad \text{or} \quad t_f \ge \delta b \tag{28}$$

Constraint for local buckling of compressed upper flange of I-column

$$\frac{b}{t_f} \le \frac{1}{\delta} = 28\varepsilon, \quad \text{or} \quad t_f \ge \delta b \tag{29}$$

3.3 Unknowns to be optimized

$$h,\ t_w,\ or\ \frac{t_w}{2},\ b,\ t_f \tag{30}$$

There are lower and upper limits for the unknowns. The minimum thickness is 5 mm, the maximum is 20mm. The minimum height and width is 80 mm, the maximum is 350 mm. The height is greater or equal to the width. At the I-column the overall buckling around both axes is considered.

3.4 Optimum design procedure

The Microsoft Excel Solver uses the Generalized Reduced Gradient (GRG2) algorithm for optimization in case of non-linear problems. The algorithm is developed by Leon Lasdon (University of Texas at Austin) and Allen Warren (Cleveland State University). The basic concept of the method is, that it search the solution with the expansion of Taylor-series besides non-linear criteria. The reduced gradient method separates two specified subset of the variable, a fundamental and a non-fundamental part. The effective method search the unconditional NLP problems with approximation. The process is repeated, until the optimization criterion is fulfilled (Hong-Tau et al. 2004).

3.5 Design data

Compression force N = 20-150 [kN]

Column length　　L = 2-10 [m]

Yield stress　　　f_y = 235, 355, 460, 690 [MPa]

Design rule EC3=Eurocode 3,

　　　　　　JRA=Japan Road Association,

　　　　　　API=American Petroleum Institute,

　　　　　　AISC=American Institute for Steel Construction.

3.6 Optimum results, comparisons

A great amount of calculations has been made. Figure 6 shows the optimum cross section areas [mm^2] in the function of the compression force [N] for the welded I-column: K=0,7; L=4 m; f_y=460 MPa; loading is changing. It shows that the API is the most liberal; EC3 and JRA are the most conservative rules. AISC is somewhere between them.
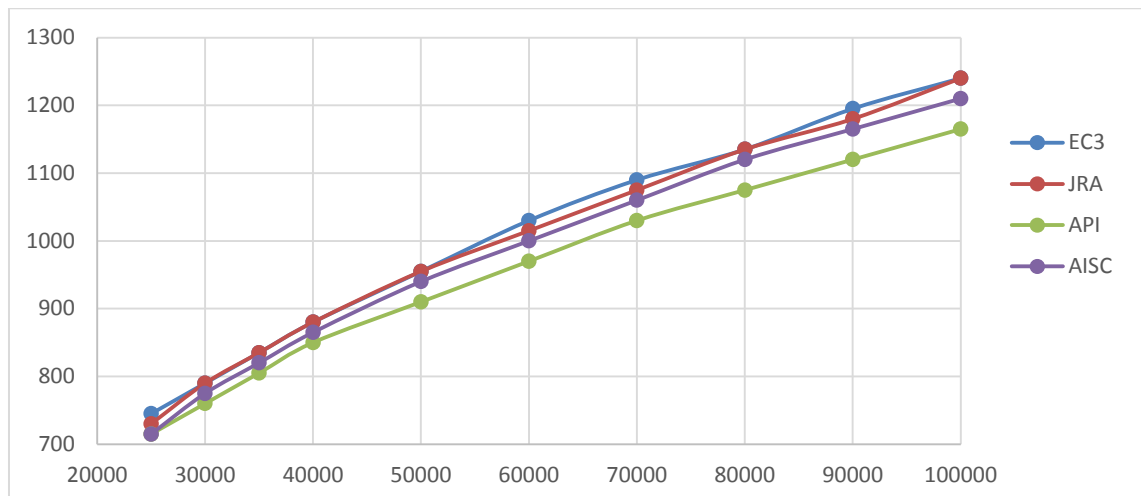

Figure 6. Optimum cross section areas [mm^2] in the function of the compression force [N] for I-column, L=4 m

Figure 7 shows the optimum cross section areas [mm^2] in the function of the compression force [N] for the welded I-column: K=0,7; L=6 m; f_y=460 MPa; loading is changing. The length is larger. There is a jump in the cross section at around 8000 N. The reason is the rounding effect.
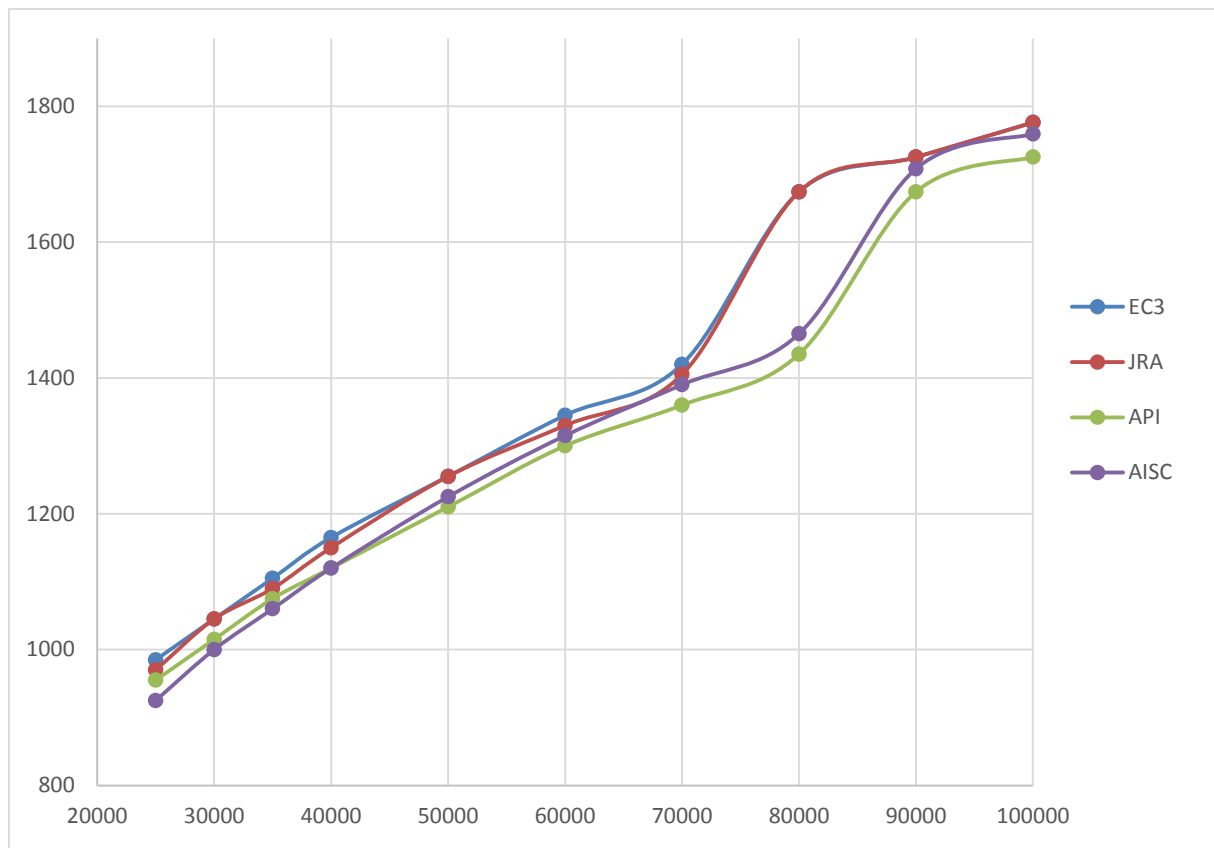

Figure 7. Optimum cross section areas [mm^2] in the function of the compression force [N] for I-column, L=6 m

Figure 8 shows the optimum cross section areas [mm^2] in the function of the yield stress [MPa] for the welded I-column: K=0,7; L=10 m; N=1500000 N. This is a surprising result. It shows the applicability of the higher strength steels. Due to the local buckling effect, one cannot get smaller cross section, increasing the yield stress up to 690 MPa. The order of the different rules is similar to the Figure 6, where the compression force changed.
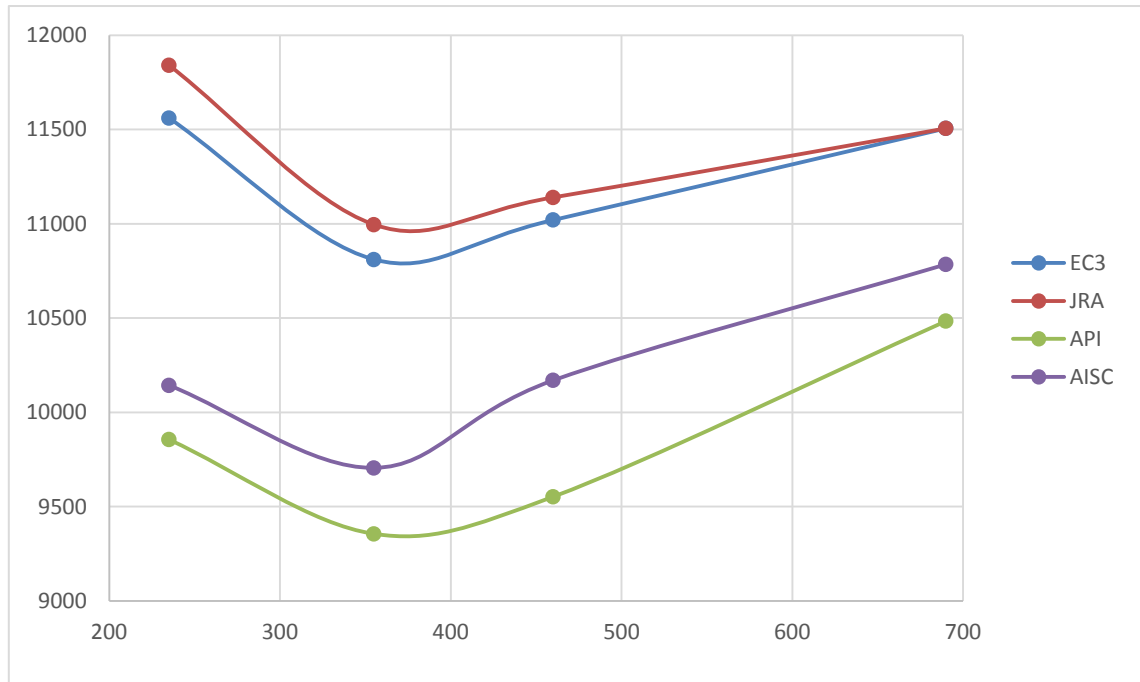
Figure 8 Optimum cross section areas [mm^2] in the function of the yield stress [MPa] for I-column, L=10 m; N=1500000 N

Figure 9 shows the optimum cross section areas [mm^2] in the function of the length [m] for the welded I-column: K=0,7; N=85000 N; f_y=235 MPa. The results are similar to Figure 7, where there are some differences at 9 m length. The reason is also the rounding effect.
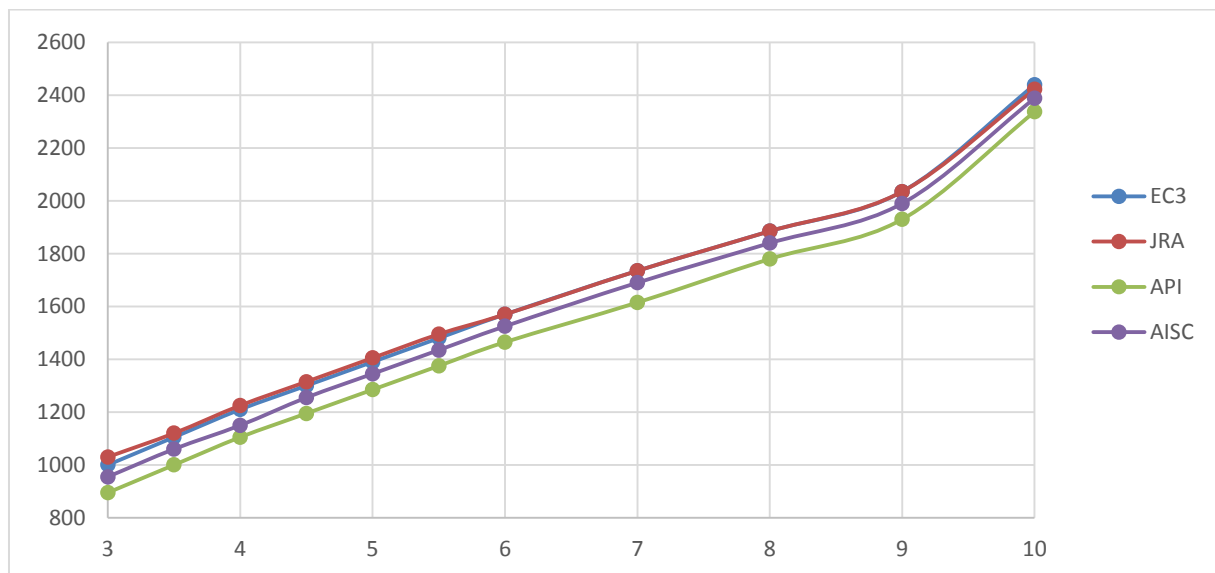

Figure 9 Optimum cross section areas [mm^2] in the function of the length [m] for I-column, N=85000 N; f_y=235 MPa

The optimization is also performed for the box column. The changing of the compression force, yield stress, length is similar.

Figure 10 shows the optimum cross section areas [mm^2] in the function of the compression force [N] for the welded box column: K=0,7; L=4 m; f_y=460 MPa; loading is changing. If we compare to Figure 7, the cross section areas are smaller for the box columns that of the I-column with 5-15 %.
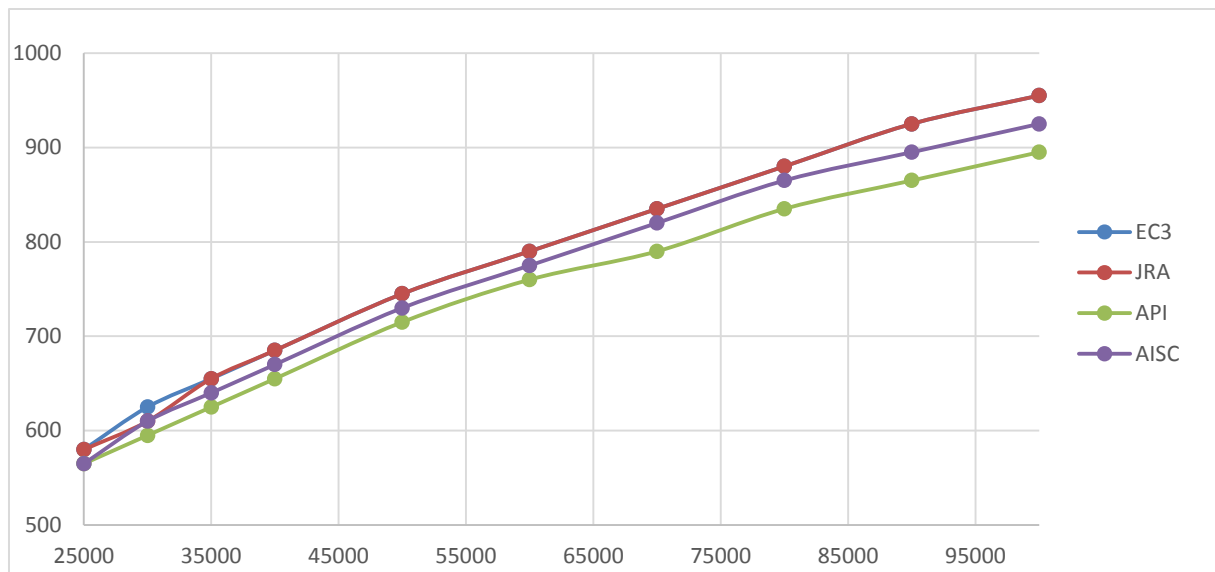

Figure 10. Optimum cross section areas [mm^2] in the function of the compression force [N] for box column, L=4 m; f_y=460 MPa

Figure 11 shows the optimum cross section areas [mm^2] in the function of the compression force [N] for the welded box column: K=0,7; L=6 m; f_y=460 MPa; loading is changing. The rounding effect is at about 7000 N.
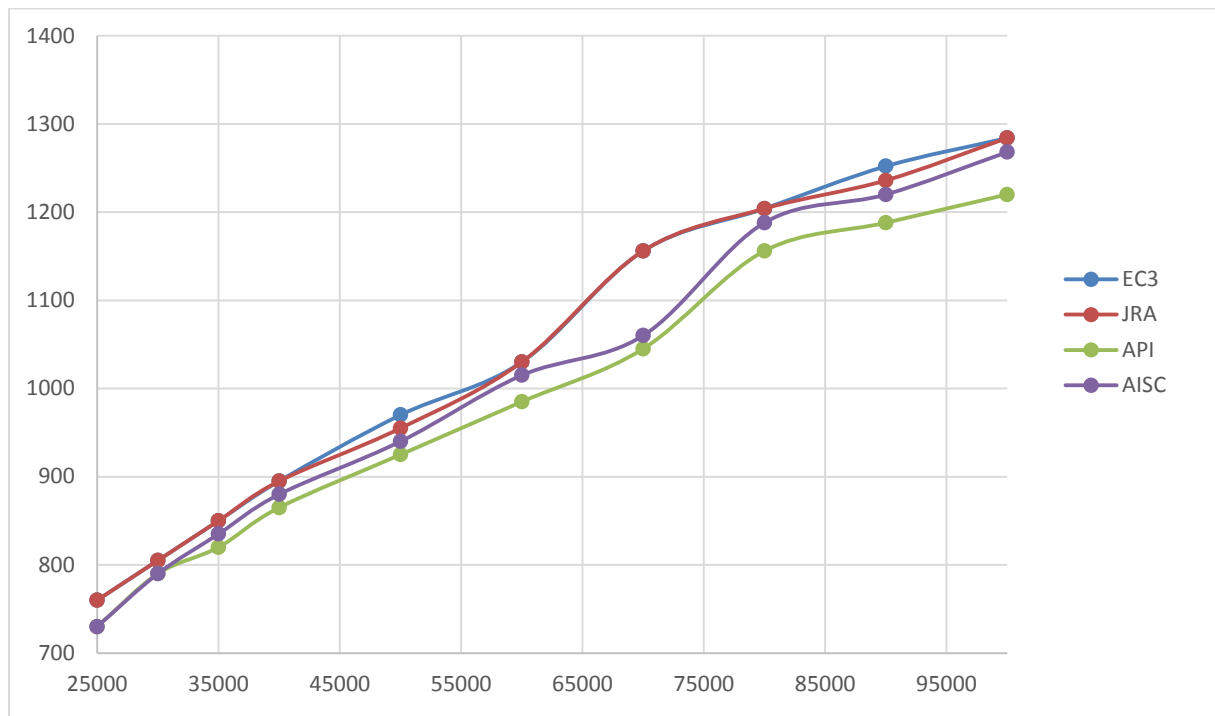

Figure 11. Optimum cross section areas [mm^2] in the function of the compression force [N] for box column, L=6 m; f_y=460 MPa

Figure 12 shows the optimum cross section areas [mm^2] in the function of yield stress [MPa] for the welded box column: K=0,7; L=10 m; N=1500000 N. The result is similar, but a bit smaller than in Figure 8 at I-columns. The box column is not so sensitive to the higher yield stress.
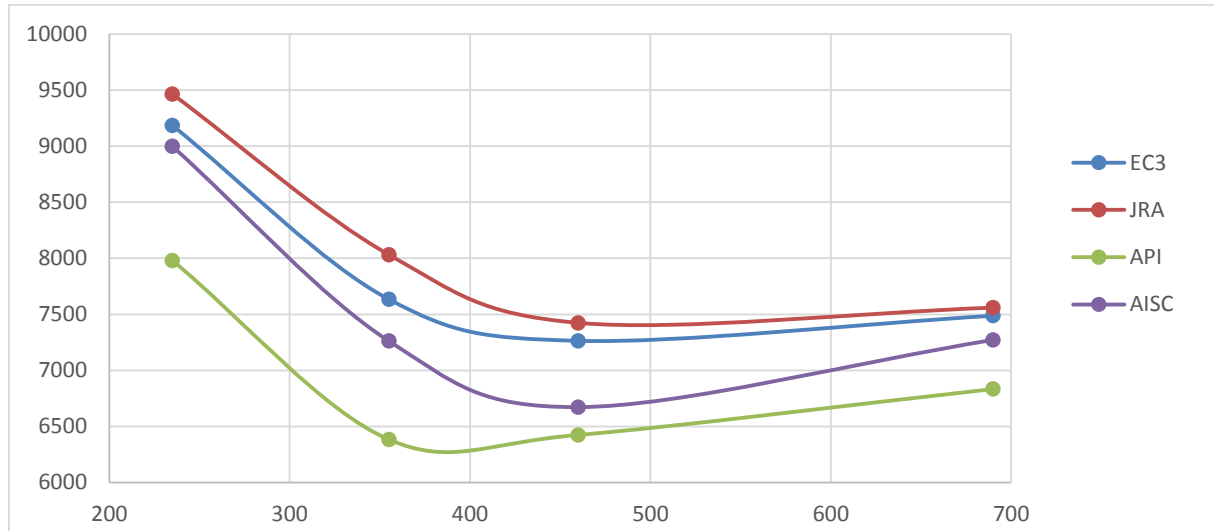

Figure 12 Optimum cross section areas [mm^2] in the function of the yield stress [MPa] for box column, L=10 m; N=1500000 N

Figure 13 shows the optimum cross section areas [mm^2] in the compression force [N] for the welded box and I-column: K=0,7; L=4 m, f_y=460 MPa. Due to the fact, that we have calculated the welded I-column for both axis, the box column is more economic. The mass saving difference is about 28 % .
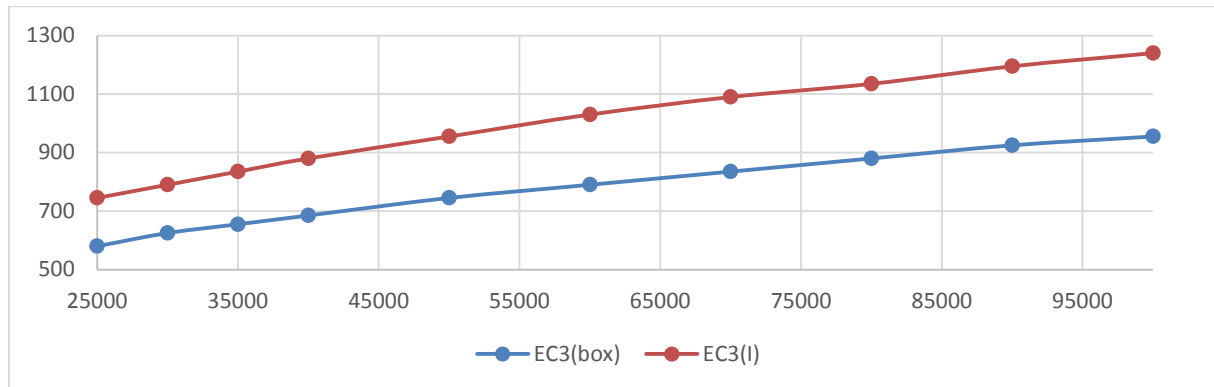

Figure 13 The optimum cross section areas [mm^2] in the function of the compression force [N] for the welded box and I-column: K=0,7; L=4 m, f_y=460 MPa.

Figure 14 shows the screenshot of the Excel Solver. Programming the overall and local stability equations, the cross section area, one can get the optimum relatively quickly.
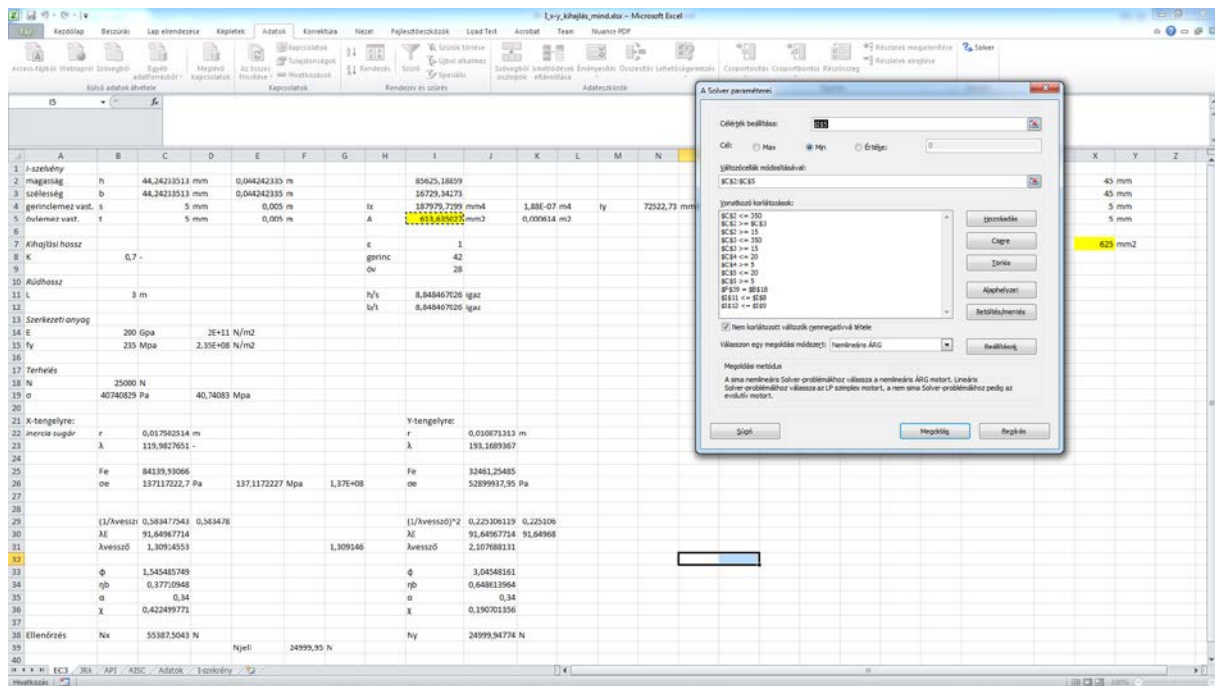
Figure 14. Screenshot of the Excel Solver using EC3 for I-column

4 Conclusions

In the optimization process the height, the width and the thickness of web and flanges have been optimized: The objective function to be minimized was the cross section, the constraints were the overall column buckling and local buckling of the web and flanges. The calculations show, that for a predesign the optimization is applicable and very useful. The Solver gives the result quickly. Building the optimization system in the Solver environment is relatively easy for the user. The welded box column is better that of the welded I-column due to the fact that the overall stability is considered at both axes. The mass saving can go up to 28% using box column. Using different standards and design rules the optimum sizes and cross sections are different. The JRA and EC3 look more conservative, the API is more liberal and the AISC is between them.

Changing the length and the compression force at the column, the cross section (the mass of the column) is not linearly but less proportional to them. The reason is probably that the local buckling does not depend on them.

The yield stress has a special effect. Increasing the yield stress from 235 MPa up to 690 MPa, first the cross sections decrease at 355 MPa, but later increase. The reason is also at the local buckling constraint and also at the overall buckling one, because of the value of $\varepsilon = \sqrt{\dfrac{235}{f_y}}$. Considering the cost of the steel one can say, that the best is the 355 MPa steel.

Acknowledgements

References

Anbarasu, M. and Murugapandian, G. (2016) "Experimental study on cold-formed steel web stiffened lipped channel columns undergoing distortional–global interaction." Materials and Structures, 10.1617/s11527-015-0586-6, 1433-1442. Online publication date: 1-Apr-2016.

Ayrton,W.E, Perry,J. (1886) On struts. The Engineer 62, p.464.

Bebiano R, Silvestre N, Camotim D (2008) GBTUL 2.0b code for buckling and vibration analysis of thin-walled members, freely available at http://www.civil.ist.utl.pt/gbt

Beer,H., Schulz,G. (1970) Bases théoriques des courbes européennes de flambement. Construction Métallique, No.3.

Braham,M., Grimault,J.P. et al. (1980) Buckling of thin-walled hollow sections. Cases of axially-loaded rectangular sections. Acier-Stahl-Steel 45, 30-36.

Chen,W.F., Atsuta,T. (1976-77) Theory of beam-columns. Vols 1-2. New York etc. McGraw Hill.

Chen,W.F., Lui,E.M. (1987) Structural stability. New York etc. Elsevier.

Chen,W.F., Lui, E.M. (1991) Stability design of steel frames. Boca Raton, Lewis Publ.

Crisan, A., Ungureanu, V., and Dubina, D. (2012) "Behaviour of cold-formed steel perforated sections in compression. Part 1—Experimental investigations." Thin-Walled Structures, 10.1016/j.tws.2012.07.016, 86-96. Online publication date: 1-Dec-2012.

Dinis, P., Young, B., and Camotim, D. (2014) "Local–distortional interaction in cold-formed steel rack-section columns." Thin-Walled Structures, 10.1016/j.tws.2013.09.010, 185-194. Online publication date: 1-Aug-2014.

Dinis, P., Young, B., and Camotim, D. (2014). "Strength, interactive failure and design of web-stiffened lipped channel columns exhibiting distortional buckling." Thin-Walled Structures, 10.1016/j.tws.2013.09.016, 195-209. Online publication date: 1-Aug-2014.

Dinis, P. and Camotim, D. (2015) "Cold-formed steel columns undergoing local–distortional coupling: Behaviour and direct strength prediction against interactive failure." Computers & Structures, 10.1016/j.compstruc.2014.09.012, 181-208. Online publication date: 1-Jan-2015.

Dubina, D., Ungureanu, V., and Crisan, A. (2013) "Experimental Evidence of Erosion of Critical Load in Interactive Buckling." Journal of Structural Engineering, 10.1061/(ASCE)ST.1943-541X.0000789, 705-716. Online publication date: 1-May-2013.

Duan,L. (1990) Stability analysis and design of steel structures. PhD Dissertation, Purdue University.

Duan,L., Chen,W.F. (1989) Design interaction equation for steel beam-columns. J. Struct.Eng ASCE 115, 1225-1243.

Ellinas,C.P.,Supple,W.J.,Walker,A.C. (1984) Buckling of offshore structures. London, Granada.

Euler,L. (1776) Determinatio onerum, quae columnae gestare valent. Acta Acad. Sci. Petrop. 2.

Eurocode 3. Part 1.1. Design of steel structures. General rules and rules for buildings. European Committee for Standardization. Brussels, 1992.

Farkas,J. (1977) The effect of residual welding stresses on the buckling strength of compressed plates. Proc. Regional Colloquium on Stability of Steel Structures, Budapest.299-306.

Farkas,J., Jármai,K. (2013) Optimum design of steel structures. Springer Verlag Berlin Heidelberg

Faulkner,D., Adamczak,J.C. et al. (1973) Synthesis of welded grillages to withstand compression and normal loads. Computers and Struct. 3, 221-246.

Gilbert, B., Savoyat, T., and Teh, L. (2012) "Self-shape optimisation application: Optimisation of cold-formed steel columns." Thin-Walled Structures, 10.1016/j.tws.2012.06.008, 173-184.

Handbook of structural stability.(1971) Column Research Council of Japan, Tokyo, Corona Publ.

He, Z., Zhou, X., Liu, Z., and Chen, M. (2014) "Post-buckling behaviour and DSM design of web-stiffened lipped channel columns with distortional and local mode interaction." Thin-Walled Structures, 10.1016/j.tws.2014.07.001, 189-203. Online publication date: 1-Nov-2014.

Hong-Tau Lee, Sheu-Hua Chen, He-Yau Kang (2004) A Study of Generalized Reduced Gradient Method with Different Search Directions, Measurement Management Journal, Vol. 1, No. 1, pp. 25-38. ISSN 1812-8572.

Kollár,L., Dulácska,E. (1984) Buckling of shells for engineers. Budapest, Akadémiai Kiadó.

Kumar, M. and Kalyanaraman, V. (2014) "Distortional Buckling of CFS Stiffened Lipped Channel Compression Members." Journal of Structural Engineering, 10.1061/(ASCE)ST.1943-541X.0001027, 04014099. Online publication date: 1-Dec-2014.

Kwon, Y. and Seo, E. (2013) "Prediction of the compressive strength of welded RHS columns undergoing buckling interaction." Thin-Walled Structures, 10.1016/j.tws.2013.03.009, 141-155. Online publication date: 1-Jul-2013.

Kwon, Y. (2014) "The development of the direct strength method for welded steel members with buckling interactions." Thin-Walled Structures, 10.1016/j.tws.2013.07.016, 121-131. Online publication date: 1-Aug-2014.

Lian, M., Su, M., and Guo, Y. (2015) "Seismic performance of eccentrically braced frames with high strength steel combination." Steel and Composite Structures, 10.12989/scs.2015.18.6.1517, 1517-1539. Online publication date: 25-Jun-2015.

Manikandan, P. and Arun, N. (2016) "Numerical Investigation on Cold-Formed Steel Lipped Channel Columns with Intermediate Web Stiffeners." Journal of The Institution of Engineers (India): Series A, 10.1007/s40030-016-0148-0, Online publication date: 16-Mar-2016.

Martins, A., Dinis, P., Camotim, D., and Providência, P. (2015) "On the relevance of local–distortional interaction effects in the behaviour and design of cold-formed steel columns." Computers & Structures, 10.1016/j.compstruc.2015.08.003, 57-89. Online publication date: 1-Nov-2015.

Martins, A., Camotim, D., Dinis, P., and Young, B. (2015) "Local–Distortional Interaction in Cold-formed Steel Columns: Mechanics, Testing, Numerical Simulation and Design." Structures, 10.1016/j.istruc.2015.10.005, 38-57. Online publication date: 1-Nov-2015.

Maquoi,R., Rondal,J. (1978) Mise en équation des nouvelles courbes européennes de flambement. Construction Métallique 15. No.1.17-30.

Naderian, H. and Ronagh, H. (2015) "Buckling analysis of thin-walled cold-formed steel structural members using complex finite strip method." Thin-Walled Structures, 10.1016/j.tws.2015.01.008, 74-83. Online publication date: 1-May-2015.

Petersen,Ch. (1980) Statik und Stabilität der Baukonstruktionen. Braunschweig-Wiesbaden, Vieweg & Sohn.

Rondal,J., Würker,K.-G. et al. (1992) Structural stability of hollow sections. Köln, Verlag TÜV Rheinland.

Sohal,I.S., Duan,L., Chen,W.F. (1989) Design interaction equations for steel members. J. Struct. Eng ASCE 115:50-1665.

Stability of metal structures. A world view. 2nd ed. Ed. Beedle,L.S. (1991) Structural Stability Research Council, Bethlehem, USA.

Timoshenko,S.P., Gere,J.M. (1961) Theory of elastic stability. 2nd ed. New York, Mc Graw Hill.

Trahair,N.S. (1993) Flexural-torsional buckling of structures. London, etc. E.&FN Spon.

Usami,T., Fukumoto,Y. (1982) Local and overall buckling of welded box columns. J.Struct.Div. Proc. ASCE 108, 525-541.

Vol'mir,A.S. (1967) Stability of deformable systems (in Russian). Moscow, Nauka.

Young, B., Silvestre, N., and Camotim, D. (2012) "Cold-Formed Steel Lipped Channel Columns Influenced by Local-Distortional Interaction: Strength and DSM Design." Journal of Structural Engineering, 10.1061/(ASCE)ST.1943-541X.0000694, 1059-1074. Online publication date: 1-Jun-2013.

Wang, Y., Li, G., Chen, S., and Sun, F. (2014) "Experimental and numerical study on the behavior of axially compressed high strength steel box-columns." Engineering Structures, 10.1016/j.engstruct.2013.10.013, 79-91. Online publication date: 1-Jan-2014.

Wang, C., Zhang, Z., Zhao, D., and Liu, Q. (2016) "Compression tests and numerical analysis of web-stiffened channels with complex edge stiffeners." Journal of Constructional Steel Research, 10.1016/j.jcsr.2015.08.013, 29-39. Online publication date: 1-Jan-2016.

Waszczyszyn,Z., Cichon,Cz., Radwanska,M. (1994) Stability of structures by finite element methods. Amsterdam, etc. Elsevier.